中國機械工程學刊第四十卷第三期第 273~285 頁(民國一百零八年)
Journal of the Chinese Society of Mechanical Engineers, Vol.40, No.3, pp 273~285 (2019)

Hierarchical Decentralized Fuzzy Sliding-Mode Control for the Path-Tracking of Differential Driven Mobile Robots

Hsiu-Ming Wu* and Mansour Karkoub**

Keywords : Differential driven mobile robot, nonlinear position control, decentralized fuzzy sliding-mode control, Lyapunov stability, virtual reference input.

ABSTRACT

The goal of this work is to achieve path-tracking of a differential driven mobile robot (DDMR) in the presence of uncertainties, saturated input, and external disturbances. To reach this goal, hierarchical decentralized fuzzy sliding-mode control (HDFSMC), including a nonlinear position control (NPC), is used to generate the desired velocity inputs of the nominal system. A decentralized fuzzy sliding-mode control (DFSMC) is also used to deal with the existence of uncertainties, saturated input and external disturbance in addition to velocity tracking. The error dynamics between the actual DDMR and the virtual reference DDMR (or the desired velocity inputs) with respect to the world frame is first established to asymptotically track the planned trajectory. Usually, the performance and stability of the closed-loop system often deteriorate because of mentioned uncertainties and exogenous inputs. A DFSMC is designed to obtain good performance including accuracy of path tracking and smoothness of the control input by exploiting some of the features of the sliding-mode control technique, e.g., excess robustness, fast convergence. First, a suitable rule table for the ith subsystem is obtained using if-then rules. Then, based on Lyapunov stability criterion, the output scaling factor is then determined. To validate the theoretical developments, computer simulations are conducted which prove the effectiveness, efficiency and robustness of the proposed scheme.

Paper Received January, 2018. Revised May, 2018. Accepted June, 2018. Author for Correspondence:Hsiu-Ming Wu

* *Assistant Professor, Department of Mechanical Engineering, National Chin-Yi University of Technology, Taichung, Taiwan41170, R.O.C.*

** *Professor, Department of Mechanical Engineering, Texas A&M University at Qatar, Doha, Qata23874*

INTRODUCTION

Motion planning of mobile robots has always been a research topic of high interests. The reasons lie in high mobility and obvious relevance in applications for mobile robots. Much research has been carried out in mechanical design, path planning and obstacle avoidance, etc. A representative few are discussed herein about derivation of the dynamic model or motion control of mobile robots. In 2010, Yue et al. (2010) presented a new dynamic model for a class of two-wheeled mobile robots and a sliding mode controller based on the adaptive gain technique to overcome the disturbances. A backstepping-based tracking control design for uncertain mobile robot systems with non-holonomic constraints is developed in (Huang, 2009). Kim and Kim (2011) solved a minimum-time trajectory planning problem for three-wheeled omnidirectional mobile robots and presented a systematic way to construct the optimal control input vector. Rubagotti et al. (2011) proposed a control strategy, which included online trajectory generation, based on harmonic potential fields and the design of sliding-mode controller for tracking both the velocity and the orientation. Chwa (2010, 2012) represented a fuzzy adaptive tracking control and a backstepping-like feedback linearization for tracking control of a wheeled mobile robot with dynamic disturbances. Moreover, in (Hou et al., 2009), a robust adaptive controller is proposed for the tracking control of an electrically driven nonholonomic mobile robot with model uncertainties that employs adaptive control approaches to attain velocity control and make use of fuzzy logic systems to learn the behavior of the unknown dynamics of the robot and the wheel actuators. Recently, smart and intelligent control technologies have been developed (see for example (Fei and Ding, 2012). In (Wai and Muthusamy), fuzzy control and neural-network techniques have been applied for robots and lead to good results. Motivated by the previous works, an intelligent control scheme with excess robustness is developed here for the path-tracking of DDMRs.

There are two types of mobile robots: differential driven (see Figure 1.) and car-like (Hwang and Chang, 2007). In the differential driven robot case, the differential velocities cause the wheels to move and/or change direction; whereas, in the car-like case, the back wheels cause the motion and the front ones change the direction. Moreover, both types have nonholonomic constraints which means they cannot move arbitrarily i.e., only move in the direction normal to the axis of the active wheels. Furthermore, most of the models used are based on laboratory scale mobile robots and only kinematics is considered that may cause part of significant dynamic behaviors missing (Kanayama et al., 1990). Hence, to establish richer and more complete mathematic model, kinematic and dynamic models with friction under nonholonomic constraints need to be taken into consideration explicitly in this study via Euler-Lagrange formulation (Fierro and Lewis, 1997).

It is known that hierarchical control architecture has been successfully applied to formation control of mobile robots (e.g., Mehrjerdi et al., 2011; Kwon and Chwa, 2012), large-scale systems (Sadati and Ramezani, 2010), manipulators (Goulet, 2001), etc. Generally speaking, hierarchical structure is suitable for the control of interconnected dynamic systems whose behaviors are affected by the dynamics among its various subsystems. Furthermore, the subsystems at both the upper and lower levels can work concurrently. On the basis of these characteristics, hierarchical architecture is utilized to achieve the path-tracking of mobile robots under prescribed trajectories. To the best of our knowledge, DFSMC with hierarchical control structure never been applied to the problem of path tracking of mobile robots in the presence of uncertainties and frictions. In this paper, the upper level generates a virtual reference input via NPC to attain the path-tracking of the DDMR. Then, the lower level reaches the velocity control through DFSMC based on the virtual reference input generated by the upper level. Certainly, control of the upper level affects the stability and performance of the lower level. Finally, each subsystem must be examined individually for the stability of the closed-loop system (e.g. Qian et al., 2008; Drakunov and Reyhanoglu, 2010; Darvishzadeh et al., 2012; Wang et al., 2007).

Motivated by the work described above, hierarchical decentralized fuzzy sliding-mode control laws (HDFSMC) for the path-tracking control of a DDMR in the presence of uncertainties, saturated input, and external disturbance are developed here. The proposed closed-loop control system includes both the kinematic and dynamic models of the DDMR. Based on the system characteristics and task, the direct and indirect states and outputs are first separated. The indirect outputs (and states) include translational and rotational velocities of the DDMR; the direct outputs (or states) are the 2D position coordinates, and orientation. Moreover, the path-tracking problem for a DDMR can be viewed as tracking a virtual reference DDMR. According to the planned task, the indirect reference input is designed via an NPC so that direct tracking error converges asymptotically to zero. Subsequently, the sliding surface using the indirect tracking error is employed to construct the DFSMC such that under appropriate conditions the asymptotic tracking of indirect output is achieved. Finally, the asymptotic tracking of both direct and indirect outputs is achieved. In short, the contributions of this study are summarized as follows: (i) the concept of virtual reference DDMR is integrated such that the desired velocity input asymptotically tracks the planned trajectory; (ii) the proposed controllers with a hierarchical structure are respectively designed based on the kinematic and dynamic models; (iii) the proposed control technique scheme (i.e., HDFSMC) has excess robustness to deal with uncertainties, saturated input, and sudden external disturbances; (iv) the stability and performance of the closed-loop system are verified via the Lyapunov stability criterion.

The paper is organized as follows. In the next section, system description and problem statement are given. In section III, path-tracking, the virtual reference input and sliding surface are designed. The controller development of DFSMC is constructed in section IV. Simulation results and corresponding discussions are given in section V. Finally, the conclusions are drawn in section VI.

SYSTEM DESCRIPTION AND PROBLEM STATEMENT

System Description

Assume to be of the unicycle type, the kinematic model of a DDMR shown in Figure 1 under nonholonomic constraints (i.e., rolling without slipping) is expressed as follows:

$$\begin{aligned} \dot{x}_w(t) &= v_w(t)\cos(\theta_w) \\ \dot{y}_w(t) &= v_w(t)\sin(\theta_w) \\ \dot{\theta}_w(t) &= \omega_w(t) \end{aligned} \tag{1}$$

where the triple $(x_w(t), y_w(t), \theta_w(t))$ denotes the position and heading angle of the vehicle with respect to two-dimensional world coordinate $X_w - Y_w$, and $v_w(t)$ and $\omega_w(t)$ are the linear and angular velocities of the DDMR with respect to world coordinate. Moreover, through Euler-Lagrange formulation the dynamic model of a DDMR is expressed as follows (Fierro and Lewis, 1997, 1998):

$$A\dot{\Omega}_R(t) + B\dot{\Omega}_L(t) = \tau_R(t) - K_f\Omega_R(t), \tag{2}$$

$$B\dot{\Omega}_R(t) + A\dot{\Omega}_L(t) = \tau_L(t) - K_f\Omega_L(t), \tag{3}$$

where $A = \left(Mr^2/4 + I_{c_g} r^2 / L^2 + I_0\right)$ and $B = \left(Mr^2/4 - I_{c_g} r^2/L^2\right)$; M and I_{c_g} are respectively the mass and the moment of inertia of the entire vehicle considering point c_g ; I_0 is the moment of inertia of the rotor/wheel system; L and r are respectively the distance between left wheel and right wheel, and the radius of the wheel; $\tau_R(t)$ and $\tau_L(t)$ are the right and left actuation torques; and K_f is the viscous friction constant. Furthermore, the relation between $v_w(t)$ and $\omega_w(t)$ and $\Omega_R(t)$ and $\Omega_L(t)$ are expressed as follows:

$$v_w(t) = r\left[\Omega_R(t) + \Omega_L(t)\right]/2, \tag{4}$$

$$\omega_w(t) = r\left[\Omega_R(t) - \Omega_L(t)\right]/L. \tag{5}$$

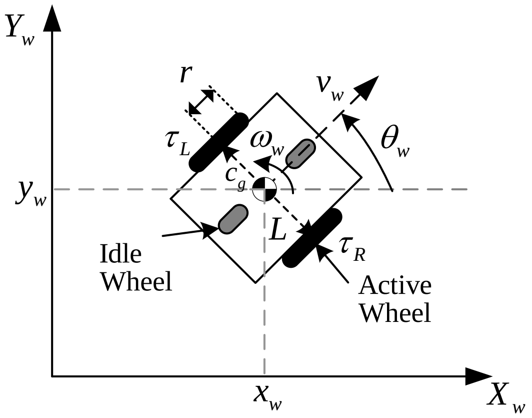

Fig. 1. Schematic description of a DDMR

To express the system (1)~(3) in a matrix form, the following states $x_1(t) = x_w(t)$, $x_2(t) = y_w(t)$, $x_3(t) = \theta_w(t)$, $x_4(t) = \Omega_R(t)$ and $x_5(t) = \Omega_L(t)$ are defined. Then, the system in matrix form is given as follows:

$$\begin{aligned} &\dot{X}_1(t) = G_1(X)V(t), \\ &\dot{X}_2(t) = F(X,t) + G_2(X,t)U(t), \\ &Y_1(t) = H_1\left[X_1(t) + \Delta X_1(t)\right], \\ &Y_2(t) = H_2\left[X_2(t) + \Delta X_2(t)\right] \end{aligned} \tag{6}$$

where $X_1^T(t) = \left[x_1(t) \quad x_2(t) \quad x_3(t)\right]$ and $X_2^T(t) = \left[x_4(t) \quad x_5(t)\right]$ are the position and velocity states, respectively; the state $X(t) = \left[X_1^T(t) \quad X_2^T(t)\right]^T \in \Re^5$; $Y_1(t) = \left[y_{1_{11}}(t) \quad y_{1_{12}}(t) \quad y_{1_{13}}(t)\right]^T \in \Re^3$ is denoted as the direct position output; $Y_2(t) = \left[y_{2_{11}}(t) \quad y_{2_{12}}(t)\right]^T \in \Re^2$ stands for the indirect velocity output; $V(t) = \left[v_w(t) \quad \omega_w(t)\right]^T \in \Re^2$ is the virtual velocity input, $U(t) = \left[u_1(t) \quad u_2(t)\right]^T = \left[\tau_R(t) \quad \tau_L(t)\right]^T \in \Re^2$ is the control input; and $H_1 \in \Re^{3\times3}$ and $H_2 \in \Re^{2\times2}$ are the output gain matrices; $\Delta X_1^T(t) = \left[\Delta x_1(t) \quad \Delta x_2(t) \quad \Delta x_3(t)\right] \in \Re^{3\times1}$ and $\Delta X_2{}^T(t) = \left[\Delta x_4(t) \quad \Delta x_5(t)\right] \in \Re^{2\times1}$ are the measurement noises. It is assumed that $\|\Delta X_1(t)\| < \|X_1(t)\|, \|\Delta X_2(t)\| < \|X_2(t)\| \forall t.$

The corresponding nominal and uncertain vector functions are described as follows:

$$\begin{aligned} &F(X,t) = \bar{F}(X) + \Delta F(X,t) \\ &G_i(X,t) = \bar{G}_i(X) + \Delta G_i(X,t), i = 1,2. \end{aligned} \tag{7a}$$

where the normal system vector functions are expressed as follows:

$$\begin{aligned} &\bar{F}(X) = \left[\bar{f}_1(X) \quad \bar{f}_2(X)\right]^T, \\ &\bar{f}_1(X) = \left(-AK_f x_4(t) + BK_f x_5(t)\right)\Big/\left(A^2 - B^2\right), \\ &\bar{f}_2(X) = \left(BK_f x_4(t) - AK_f x_5(t)\right)\Big/\left(A^2 - B^2\right); \\ &\bar{G}_1(X) = \begin{bmatrix} \cos\theta_w & 0 \\ \sin\theta_w & 0 \\ 0 & 1 \end{bmatrix}, \\ &\bar{G}_2 = \begin{bmatrix} A\Big/\left(A^2 - B^2\right) & -B\Big/\left(A^2 - B^2\right) \\ -B\Big/\left(A^2 - B^2\right) & A\Big/\left(A^2 - B^2\right) \end{bmatrix}. \end{aligned} \tag{7b}$$

The uncertain system functions are defined as follows:

$$\begin{aligned} &\Delta F^T(X,t) = \left[\Delta f_1(X,t) \quad \Delta f_2(X,t)\right], \\ &\Delta G_1(X,t) = \begin{bmatrix} \Delta g_{1_{11}}(X,t) & \Delta g_{1_{12}}(X,t) \\ \Delta g_{1_{21}}(X,t) & \Delta g_{1_{22}}(X,t) \\ \Delta g_{1_{31}}(X,t) & \Delta g_{1_{32}}(X,t) \end{bmatrix}, \\ &\Delta G_2(X,t) = \begin{bmatrix} \Delta g_{2_{11}}(X,t) & \Delta g_{2_{12}}(X,t) \\ \Delta g_{2_{21}}(X,t) & \Delta g_{2_{22}}(X,t) \end{bmatrix}. \end{aligned} \tag{7c}$$

In addition, the output gain matrices are given as follows:

$$H_1 = I_3, H_2 = \begin{bmatrix} r/2 & r/2 \\ r/L & -r/L \end{bmatrix}. \tag{8a}$$

The nominal system outputs are as follows:

$$\begin{aligned} &Y_1^T(t) = \left[x_w(t) \quad y_w(t) \quad \theta_w(t)\right], \\ &Y_2^T(t) = \left[v_w(t) \quad \omega_w(t)\right]. \end{aligned} \tag{8b}$$

The first line of (6) with uncertainty can be written as follows:

$$\dot{X}(t) = A(X) + B(X)U(t) + C(X,t) \tag{8c}$$

where $A(X) \in \Re^5$ and $B(X) \in \Re^{5\times2}$ denote the nominal system; $U(t) = \left[\tau_R(t) \quad \tau_L(t)\right]^T \in \Re^2$ is the control torque; $C(X,t) \in \Re^5$ denotes the nonlinear time-varying uncertainties caused by parameter variations, e.g., $\Delta f_i(X,t)$ and $\Delta G_i(X,t)$ for $i = 1,2,$ saturated input, and external disturbance. The system (8c) is employed to design the DFSMC.

Remark 1: The uncertain control gain matrix, i.e., $\Delta G_i(X,t), i = 1,2.$ can be considered as input disturbances, e.g., dead-zone, backlash and hysteresis, or external disturbance. In this paper, the states, i.e., $X(t)$, are assumed to be available. The outputs are chosen from the corresponding states. Hence, the measurement noise affects to the state not the output. This is the reason for the description of the 2nd line of (6). Furthermore, unknown friction is considered as uncertainties shown in the first line of (7c).

Problem Statement

Before discussing the problem statement, tracking errors are defined as follows:

$$E_i(t) = R_i(t) - Y_i(t),\ i = 1, 2. \tag{9}$$

The objective is to design the control input for the DDMR system (1)~(5) or (6)~(8) such that the system output $Y_1(t)$ tracks a reference input $R_1(t) = \begin{bmatrix} x_r(t) & y_r(t) & \theta_r(t) \end{bmatrix}^T$ and $Y_2(t)$ also tracks the virtual reference input $R_2(t) = \begin{bmatrix} v_r(t) & \omega_r(t) \end{bmatrix}^T$ (refer to Figure 2). At the beginning, the virtual reference input $R_2(t)$ is designed by a nonlinear position control such that the system output of velocity $Y_2(t)$ asymptotically drives the system output of position $Y_1(t)$ to converge to the reference input $R_1(t)$ as close as possible. Due to the existence of uncertainties, saturated input, and external disturbance, the decentralized fuzzy sliding mode control (DFSMC), i.e., $U(t)$, is also designed such that under suitable conditions the system output of position $Y_1(t)$ asymptotically tracks the virtual reference input $R_1(t)$. In summary, the approach of $Y_2(t)$ to $R_2(t)$ makes the output $Y_1(t)$ approach $R_1(t)$. Finally, the simulations for the system in the presence of uncertainties is applied to evaluate the effectiveness and robustness of the proposed control.

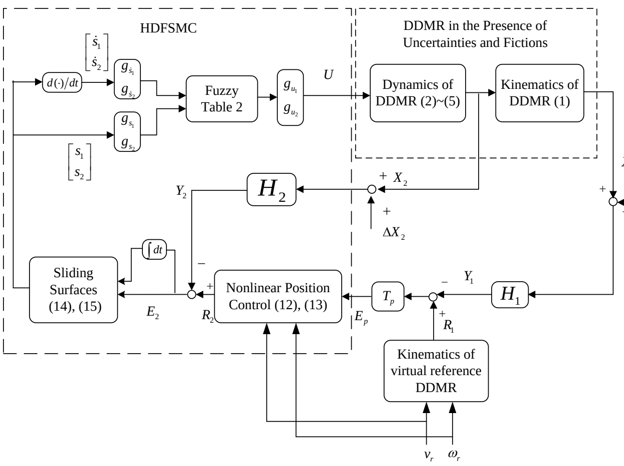

Figure 2. Control block diagram of the overall DDMR system.

PATH-TRACKING, VIRTUAL REFERENCE INPUT AND SLIDING SURFACES

The path-tracking problem for a DDMR is equivalent to the path-tracking problem of the virtual reference input (Kanayama, 1990; Egerstedt, 2010). The tracking position error between the virtual reference DDMR and the actual DDMR with respect to the world frame is expressed as follows (cf. Figure 3):

$$\begin{aligned} E_p(t) &= \begin{bmatrix} e_1(t) \\ e_2(t) \\ e_3(t) \end{bmatrix} = T_p E_1(t) \\ &= \begin{bmatrix} \cos\theta_w & \sin\theta_w & 0 \\ -\sin\theta_w & \cos\theta_w & 0 \\ 0 & 0 & 1 \end{bmatrix} \begin{bmatrix} e_x(t) \\ e_y(t) \\ e_\theta(t) \end{bmatrix} \end{aligned} \tag{10}$$

where $E_1(t) = \begin{bmatrix} e_x(t) & e_y(t) & e_\theta(t) \end{bmatrix}^T$ is denoted as the path-tracking error of the DDMR, and T_p is the transformation matrix between the virtual reference DDMR and the actual DDMR. Hence, time derivative of the position error (10) with the relations $\dot{x}_r(t) = v_r(t)\cos(\theta_r)$, $\dot{y}_r(t) = v_r(t)\sin(\theta_r)$ and $\dot{\theta}_r(t) = \omega_r(t)$ can be obtained as follows:

$$\begin{aligned} \dot{e}_1(t) &= \omega_w(t)e_2(t) + v_r(t)\cos e_3(t) - v_w(t) \\ \dot{e}_2(t) &= -\omega_w(t)e_1(t) + v_r(t)\sin e_3(t) \\ \dot{e}_3(t) &= \omega_r(t) - \omega_w(t) \end{aligned} \tag{11}$$

where $v_r(t)$ and $\omega_r(t)$ are linear and angular velocities of the virtual reference DDMR that are assumed to be bounded and have bounded derivatives. If we consider only the kinematic model (1) with a velocity input, the kinematic model is asymptotically stable with respect to a virtual reference trajectory. Based on Lyapunov stability theory, a velocity control input (i.e., virtual reference input $R_2(t)$ in Figure 3) is designed as follows.

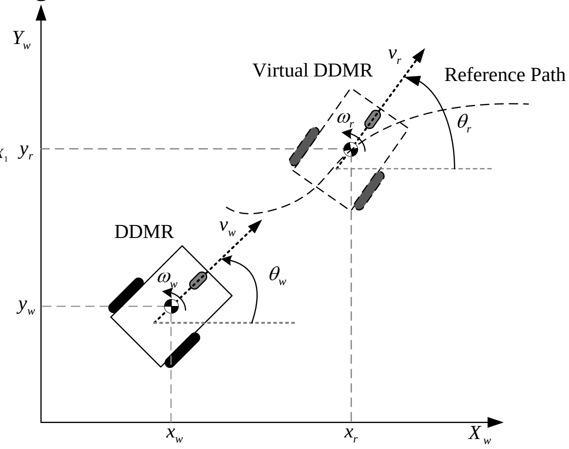

Figure 3. Path-tracking of a virtual reference DDMR

Lemma 1: The virtual reference input $R_2(t) = \left[v_w(t) \quad \omega_w(t) \right]^T$ is designed as follows:

$$v_w(t) = v_r(t) \cos e_3(t) + \gamma_1 e_1(t) \tag{12}$$

$$\omega_w(t) = \omega_r(t) + v_r(t) e_2(t) + \gamma_2 e_2^2(t) \sin e_3(t) \tag{13}$$

where γ_1 and γ_2 are positive constants which are related to the system performance. Then, $e_1(t)$, $e_2(t)$ and $e_3(t) \to 0$, as $t \to \infty$.

Proof: See Appendix A.

Then, a decentralized fuzzy sliding-mode controller (DFSMC) is designed and discussed so that virtual reference input $R_2(t)$ is tracked by $Y_2(t)$ as shown in the next section. However, before discussing the DFSMC, the sliding surfaces are defined as follows:

$$s_1(t) = k_{p_1} e_v(t) + k_{i_1} \int e_v(t) dt \tag{14}$$

$$s_2(t) = k_{p_2} e_\omega(t) + k_{i_2} \int e_\omega(t) dt \tag{15}$$

where $e_v(t) = v_r(t) - v_w(t)$ and $e_\omega(t) = \omega_r(t) - \omega_w(t)$, k_{p_1}, k_{p_2}, k_{i_1} and $k_{i_2} > 0$ are assigned such that sliding surfaces $s_1(t)$ and $s_2(t)$ are stable.

Then, the derivatives of these two sliding surfaces are expressed as follows:

$$\begin{aligned} \dot{s}_1(t) &= k_{p_1} \dot{e}_v(t) + k_{i_1} e_v(t) \\ &= k_{p_1} \left[\dot{v}_r(t) - \frac{r}{2} \begin{pmatrix} a_4(X) + a_5(X) + (b_{41} + b_{51}) u_1(t) \\ +(b_{42} + b_{52}) u_2(t) + c_4(X,t) + c_5(X,t) \end{pmatrix} \right] \\ &+ k_{i_1} e_v(t) \end{aligned} \tag{16a}$$

$$\begin{aligned} \dot{s}_2(t) &= k_{p_2} \dot{e}_w(t) + k_{i_2} e_w(t) \\ &= k_{p_2} \left[\dot{\omega}_r(t) - \frac{r}{L} \begin{pmatrix} a_4(X) - a_5(X) + (b_{41} - b_{51}) u_1(t) \\ +(b_{42} - b_{52}) u_2(t) + c_4(X,t) - c_5(X,t) \end{pmatrix} \right] \\ &+ k_{i_2} e_w(t) \end{aligned} \tag{16b}$$

The following property about "uniform ultimate boundedness (UUB)" is given:

Definition 1 (Khalil, 1996): The solutions of a dynamic system are said to be UUB if there exist positive constants υ and κ, and for every $\delta \in (0, \kappa)$ there is a positive constant $T = T(\delta)$, such that $\|x(t_0)\| < \delta \Rightarrow \|x(t)\| \le \upsilon$, $\forall t \ge t_0 + T$.

Remark 2: In this paper, $\dot{s}_1(t)$ and $\dot{s}_2(t)$ are respectively substituted by $\dot{s}_1(t) = \left[s_1(kT_s) - s_1((k-1)T_s) \right] / T_s$ and $\dot{s}_2(t) = \left[s_2(kT_s) - s_2((k-1)T_s) \right] / T_s$, where T_s denotes the sampling time. In general, the smaller the sampling time T_s is, the more accurate these time derivatives are. The approximation error between them is regarded as part of the uncertainties.

FUZZY SLIDING MODE CONTROL

Using fuzzy logic systems for control applications has many advantages e.g., flexible, model-free and excess robustness, etc. One important contribution of fuzzy systems theory is to provide a systematic procedure for transforming a set of linguistic rules into a nonlinear mapping. The fuzzy logic subsystem *i* for the DFSMC in Figure 4 performs a mapping from $X_i \in \Re^2$ to $\Re$. There are *l* fuzzy control rules and the upper script *k* denotes the *kth* fuzzy rule:

$$\text{IF } \bar{s}_i(t) \text{ is } F_{1_i}^k \text{ and } \dot{\bar{s}}_i(t) \text{ is } F_{2_i}^k, \text{ THEN } \bar{u}_i(t) \text{ is } G_i^k \tag{17}$$

where $x_i(t) = \left[\bar{s}_i(t) \quad \dot{\bar{s}}_i(t) \right]^T \in X_i \subset \Re^2$, with $\bar{s}_i(t) = g_{s_i} s_i(t)$, $\dot{\bar{s}}_i(t) = g_{\dot{s}_i} \dot{s}_i(t)$, and $\bar{u}_i(t) \in V_i \subset \Re$ are the input and output of the fuzzy logic subsystem *i*, respectively; $F_{j_i}^k (1 \le i, j \le 2, 1 \le k \le l)$ and G_i^k are labels of sets in X_i and V_i, respectively. The parameters g_{s_i} and $g_{\dot{s}_i}$ are chosen such that $\bar{s}_i(t)$ and $\dot{\bar{s}}_i(t) \in [-1, 1]$. The fuzzy inference engine performs a mapping from fuzzy sets in $X_i \subset \Re^2$ to fuzzy sets in $V_i \subset \Re$, based on the fuzzy IF-THEN rules in the fuzzy rule base and the compositional rule of inference. Let A_{x_i} be an arbitrary fuzzy set in X_i. The fuzzifier maps a crisp point $X_i(t)$ into a fuzzy set A_{x_i} in X_i. The center-average defuzzifier maps a fuzzy set in V_i to a crisp point in V_i.

The output of the DFSMC is then designed as follows:

$$\begin{aligned} u_i(t) &= g_{u_i} \bar{u}_i(t) \\ &= g_{u_i} \left[\bar{s}_i(t) + \Delta_i(t) \operatorname{sgn}(\bar{s}_i) \right] \operatorname{sgn}(\tilde{b}_i(s_1, s_2)), \; i = 1, 2. \end{aligned} \tag{18}$$

where $\bar{u}_i(t)$ is the fuzzy variable of $u(t)$ and $\Delta_i(t) > 0$, $i = 1, 2$ $\forall t$. Also

$\tilde{b}_1(s_1, s_2) = s_1 k_{p_1} r (b_{41} + b_{51}) / 2 + s_2 k_{p_2} r (b_{41} - b_{51}) / L$,

$\tilde{b}_2(s_1, s_2) = s_1 k_{p_1} r (b_{42} + b_{52}) / 2 + s_2 k_{p_2} r (b_{42} - b_{52}) / L$.

Moreover, it is assumed that the output scaling factors satisfy the following inequalities:

$$\begin{aligned} &g_{u_1} \; ? \; [\text{illegible}]_1(X,t)| \quad l_1 / [\text{illegible}](s_1, s_2) \mathrm{D}_1(t) \; , \\ &g_{u_2} \; ? \; [\text{illegible}]_2(X,t)| \quad l_2 / [\text{illegible}](s_1, s_2) \mathrm{D}_2(t) \; . \end{aligned} \tag{19}$$

where

$$h_1(X,t) \ge k_{p_1}\left[\dot{v}_r(t) - r\left(a_4(X) + a_5(X) + c_4(X,t) + c_5(X,t)\right)/2\right] + k_{i_1}e_v(t), \quad (20)$$

$$h_2(X,t) \ge k_{p_2}\left[\dot{\omega}_r(t) - r\left(a_4(X) - a_5(X) + c_4(X,t) - c_5(X,t)\right)/L\right] + k_{i_2}e_w(t). \quad (21)$$

The following theorem discusses the properties of the DFSMC.

Theorem 1: Consider the DDMR system (6) with the known upper bounds (19) together with inequalities (20) and (21). Applying (18) to the system (6), gives the finite time to reach the sliding surfaces (14) and (15), and leads to the asymptotical tracking stability.

Proof: See the *Appendix B.*

Corollary 1: If the inequalities (19), (20) and (21) are satisfied outside of the following convex set:

$$D = \left\{ s_i(t) \middle| |s_i(t)| \le d_{s_i}, i = 1,2 \right\} \quad (22)$$

where d_{s_i} are positive constants dependent on the upper bound of uncertainty, then the operating point reaches a convex set (22) in a finite time and $\{s_i(t), u_i(t)\}, i = 1,2,$ are UUB.

The corresponding three scaling factors (or control parameters) g_{s_i}, $g_{\dot{s}_i}$ and g_{u_i} are discussed as follows. Inequality (19) implies that the output scaling factor should be greater than the upper bound of the system gains, control gains, and uncertainty. In the beginning, the scaling factor is chosen from a suitable small set of values. A larger value is then applied to improve the system performance based on the system response. When a larger output scaling factor is chosen, smaller tracking error is achieved. Moreover, transient (or unstable) response may occur due to the constraints on the rate of the control input. It is worth noting that oscillatory response often occurs after transient period.

Based on the input-output data, it is assumed that $\dot{s}_i(t)$ increases as $u_i(t) = g_{u_i}\overline{u}_i(t)$ decreases, and if $s_i(t) > 0$ then increasing $u_i(t)$ will result in decreasing $s_i(t)\dot{s}_i(t)$ and if $s_i(t) < 0$ then decreasing $u_i(t)$ will result in decreasing $s_i(t)\dot{s}_i(t)$. That is, the control input $u_i(t)$ is designed in an attempt to satisfy the inequality $s_i(t)\dot{s}_i(t) < 0, i = 1,2,$ which results in decrease of Lyapunov function $V(t) = \sum_{i=1}^{2} s_i^2(t)/2,$ i.e., $\dot{V}(t) < 0.$

The fuzzy variables $\overline{s}_i(t) = g_{s_i}s_i(t)$ and $\dot{\overline{s}}_i(t) = g_{\dot{s}_i}\dot{s}_i(t), i = 1,2$ are quantized into the following eleven qualitative fuzzy variables (i.e., $l = 11$): (i) Positive Huge (PH), (ii) Positive Big (PB), (iii) Positive Medium (PM), (iv) Positive Small (PS), (v)Positive Infinitesimal (PI), (vi)Zero (ZE), (vii) Negative Infinitesimal (NI), (viii) Negative Small (NS), (ix) Negative Medium (NM), (x) Negative Big (NB), and (xi) Negative Huge (NH). It is not necessary that all eleven fuzzy rules are selected. A smaller fuzzy rule set (e.g., $l = 7$) may lead to acceptable performance (e.g., Hwang, 2007). There are many types of membership functions, some of which are bell shaped, trapezoidal shaped, and triangular shaped, etc. The triangular type in Figure 5 is used in this paper. In summary, the linguistic rule of the *ith* DFSMC is shown in Table 1 by which the center of gravity method is employed to form a look-up Table 2 that directly relates the inputs $\overline{s}_i(t)$ and $\dot{\overline{s}}_i(t)$ to the output $u_i(t)$. The control actions of the diagonal terms in Table 1 are ZE. This arrangement is similar to a sliding-mode controller that has a sliding surface. In addition, the control actions of the upper triangle terms are from NI to NH, and those of the lower triangle terms are from PI to PH; therefore, it is skew-symmetric.

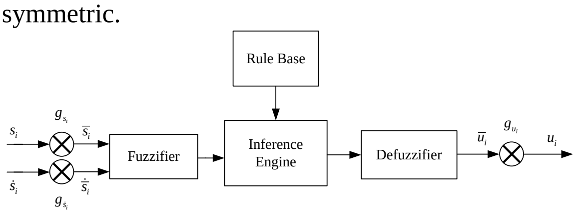

Figure 4. Basic configuration of the *ith* fuzzy logic system

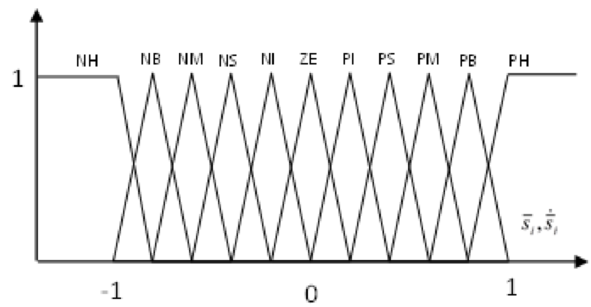

Figure 5. Membership functions with triangular type

Finally, the proposed HDFSMC is summarized as follows:

Step 1: Obtain the nominal model of a DDMR with kinematic constraint through Euler-Lagrange formulation, i.e., $\overline{F}(X)$ and $\overline{G}_i(X), i = 1,2.$

Step 2: Assign the linear and angular velocity of a virtual reference DDMR (i.e., $v_r(t)$ and $\omega_r(t)$) and then determine the direct reference input $R_1(t)$.

Step 3: Design the indirect reference input $R_2(t)$ (i.e., $v_w(t)$ and $\omega_w(t)$) with proper control parameters γ_1 and γ_2 by NPC from the error dynamics between virtual reference DDMR and actual DDMR.

Step 4: Assign the appropriate coefficients k_{p_1}, k_{p_2}, k_{i_1} and k_{i_2} of the sliding surfaces (14) and (15). Then, select two input scaling factors (i.e.,

g_{s_1} and g_{s_2}) such that values of the sliding surfaces are located in $[-1,1]$.

Step 5: Obtain the difference between the sliding surface values to substitute in the derivative of the sliding surface. Also, assign two suitable input scaling factors (i.e., $g_{\dot{s}_1}$ and $g_{\dot{s}_2}$) such that the values are located between -1 and 1.

Step 6: Establish appropriate Look-up table as in Table 2 based on *l* fuzzy control rules of (17).

Step 7: Properly select output scaling factors g_{u_1} and g_{u_2} which meet inequality (19)~(21) for the upper bound of the system gains.

Step 8: Go back to *Step 3* and *Step 4* to tune the control parameters again if performance is not acceptable.

Table 1. Rule table of the *ith* DFSMC.

$\bar{s}_i$ \ $\dot{\bar{s}}_i$	PH	PB	PM	PS	PI	ZE	NI	NS	NM	NB	NH
NH	ZE	NI	NS	NM	NM	NB	NB	NB	NH	NH	NH
NB	PI	ZE	NI	NS	NM	NM	NB	NB	NB	NH	NH
NM	PS	PI	ZE	NI	NS	NM	NM	NB	NB	NB	NH
NS	PM	PS	PI	ZE	NI	NS	NM	NM	NB	NB	NB
NI	PM	PM	PS	PI	ZE	NI	NS	NM	NM	NB	NB
ZE	PB	PM	PM	PS	PI	ZE	NI	NS	NM	NM	NB
PI	PB	PB	PM	PM	PS	PI	ZE	NI	NS	NM	NM
PS	PB	PB	PB	PM	PM	PS	PI	ZE	NI	NS	NM
PM	PH	PB	PB	PB	PM	PM	PS	PI	ZE	NI	NS
PB	PH	PH	PB	PB	PB	PM	PM	PS	PI	ZE	NI
PH	PH	PH	PH	PB	PB	PB	PM	PM	PS	PI	ZE

Table 2. Look-up table of the *ith* DFSMC.

$\bar{s}_i$ \ $\dot{\bar{s}}_i$	1.0	0.8	0.6	0.5	0.2	0	-0.2	-0.5	-0.6	-0.8	-1.0
-1.0	0.0	-0.05	-0.2	-0.5	-0.7	-0.8	-0.9	-0.95	-1.0	-1.0	-1.0
-0.8	0.05	0.0	-0.05	-0.2	-0.5	-0.7	-0.8	-0.9	-0.95	-1.0	-1.0
-0.6	0.2	0.05	0.0	-0.05	-0.2	-0.5	-0.7	-0.8	-0.9	-0.95	-1.0
-0.5	0.5	0.2	0.05	0.0	-0.05	-0.2	-0.5	-0.7	-0.8	-0.9	-0.95
-0.2	0.7	0.5	0.2	0.05	0.0	-0.05	-0.2	-0.5	-0.7	-0.8	-0.9
0	0.8	0.7	0.5	0.2	0.05	0.0	-0.05	-0.2	-0.5	-0.7	-0.8
0.2	0.9	0.8	0.7	0.5	0.2	0.05	0.0	-0.05	-0.2	-0.5	-0.7
0.5	0.95	0.9	0.8	0.7	0.5	0.2	0.05	0.0	-0.05	-0.2	-0.5
0.6	1.0	0.95	0.9	0.8	0.7	0.5	0.2	0.05	0.0	-0.05	-0.2
0.8	1.0	1.0	0.95	0.9	0.8	0.7	0.5	0.2	0.05	0.0	-0.05
1.0	1.0	1.0	1.0	0.95	0.9	0.8	0.7	0.5	0.2	0.05	0.0

SIMULATIONS AND DISCUSSIONS

To evaluating the performance of the proposed control, the simulations for a planned trajectory tracking of a DDMR are performed. First, $v_r(t) = 0.8\,m/\mathrm{s}$ and $\omega_r(t) = 0.8\cos(t)\,rad/\mathrm{s}$ are selected so that a planned trajectory $R_1(t)$ is generated for the virtual reference DDMR. Furthermore, the initial position and heading angle of the virtual DDMR and actual DDMR are chosen as $\{0.5,-2.5,\pi/3\}$ and $\{-1,-2,0\}$, respectively. The system and suitable control parameters are given in Table 3. Direct output of position $Y_1(t)$, indirect output of velocity $Y_2(t)$ and the corresponding responses in the absence of uncertainties are shown in Figure 6. From these responses, it is clear that the proposed control leads to excellent performances. Furthermore, Figure 7 shows the corresponding responses of the DDMR system with uncertainties presented in the system. In the simulations, the following multiplicative form of uncertainties for the system functions and the additive form for the measurement noises are considered to verify the robustness of the proposed controller.

$$\Delta f_1(X,t) = \bar{f}_1(X)\left[0.02\cos(10t)\sin(4x_1) - 0.06\sin(20x_2) + 0.5\sin(100t)\right]$$

$$\Delta f_2(X,t) = \bar{f}_2(X)\left[-0.04x_2\sin(2t) + 0.3\sin(50tx_4)\right]$$

$$\Delta G_1(X,t) = \bar{G}_1(X)\begin{bmatrix} 0.02x_3\sin(t) - 0.4\cos(80t) & 0 \\ -0.2\cos(5tx_2) & 0 \\ 0 & 0.02\sin(100t) \end{bmatrix}$$

$$\Delta G_2(X,t) = \bar{G}_2(X)\begin{bmatrix} 0.02\cos(10t) - 0.06\sin(20x_3) + 0.5\sin(100t) & 0 \\ 0 & -0.04x_4\sin(0.1t) + 0.3\cos(50tx_5) \end{bmatrix}$$

$$\Delta X_1(t) = \left[0.08\cos(5x_5)\sin(20t) \quad 0.04\cos(5x_2)\sin(10x_5) \quad -0.04\cos(5x_2)\sin(80t)\right]^T$$

$$\Delta X_2(t) = [0.1\cos(10tx_5)\sin(5x_4) \quad -0.06\sin(5t)\cos(10x_5)]^T. \tag{23}$$

It is shown that the HDFSMC exhibits good level of robustness in spite of the relatively large uncertainties (refer to each last part of the multiplicative form). The responses for larger uncertainties are similar to that in Figure 7, however, for brevity, they are omitted. Furthermore, for practical consideration, the response for the saturated control inputs $\tau_R(t)$ and $\tau_L(t)$ of 5 *Nm* is presented in Figure 8, which is still satisfactory. To further investigate the robustness of the proposed control scheme, sudden torques of 3 *Nm* are injected into the right and left wheels for a period of 0.5 seconds at $t = 3$s and $t = 8$s (i.e., the durations 3~3.5 and 8~8.5s). Under the same conditions described in Figure 8, the corresponding response is shown in Figure 9. It can be clearly seen that the responses of the path-tracking are still satisfactory which proves the robust performance of the proposed control scheme.

Table 3. System and control parameters.

Symbol	Description	Value
M	Mass of the entire vehicle considering point c_g	10 *kg*
I_{c_g}	Moment of Inertial of the entire vehicle considering point c_g	1 kgm^2
L	Distance between left	0.35 *m*

	wheel and right wheel	
r	Radius of Wheels	$0.035\ m$
I_0	Moment of Inertial of rotor/wheel system	$0.001\ kgm^2$
K_f	Viscous friction constant.	$0.0072\ Nm \cdot \sec/rad$
γ_1, γ_2	Control parameters	2,10
k_{p_1}, k_{p_2}	Proportional Gains 1,2	100,100
k_{i_1}, k_{i_2}	Integration Gains 1,2	2.1,10.2
g_{s_1}, g_{s_2}	Input scaling factors	0.001,0.001
$g_{\dot{s}_1}, g_{\dot{s}_2}$	Input scaling factors	0.02,0.02
g_{u_1}, g_{u_2}	Output scaling factors	20,20

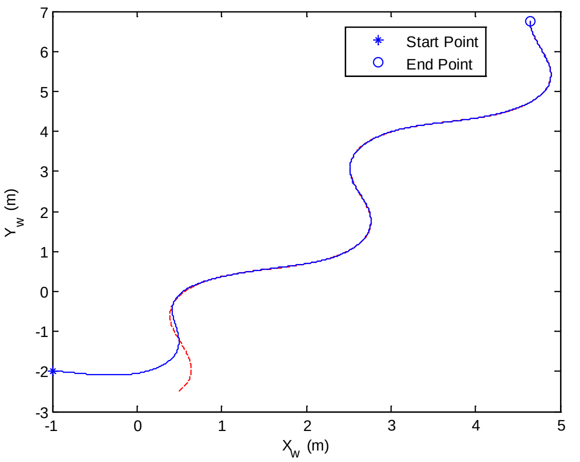

(a) $(x_w(t), y_w(t))(-)$ and $(x_r(t), y_r(t))(--)$.

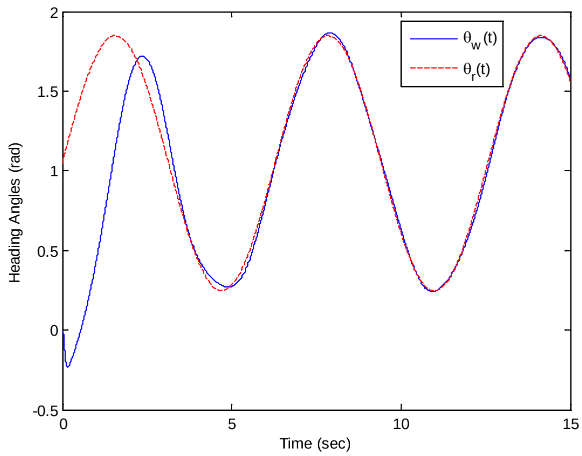

(b) $\theta_w(t)(-)$ and $\theta_r(t)(--)$.

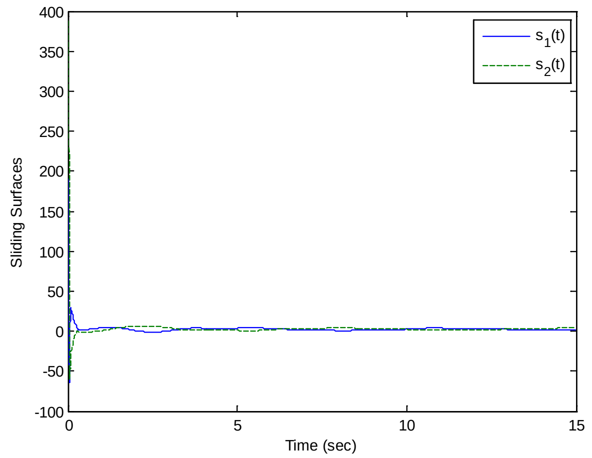

(c) $s_1(t)(-)$ and $s_2(t)(--)$.

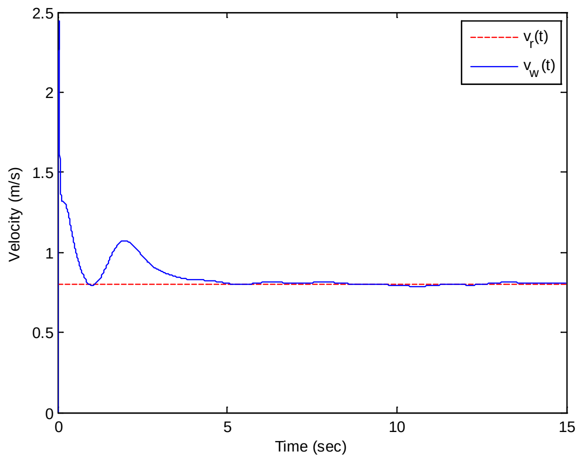

(d) $v_r(t)(--)$ and $v_w(t)(-)$.

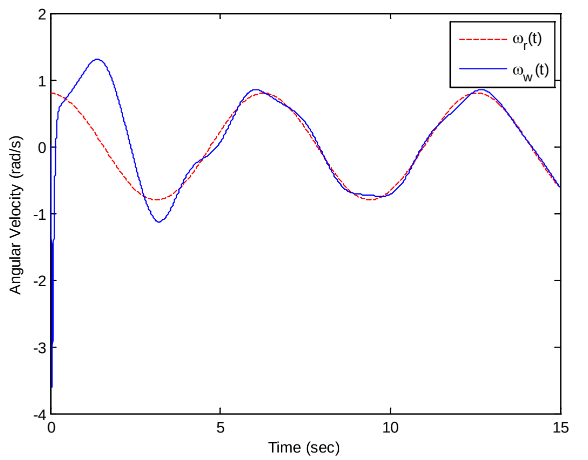

(e) $\omega_r(t)(--)$ and $\omega_w(t)(-)$.

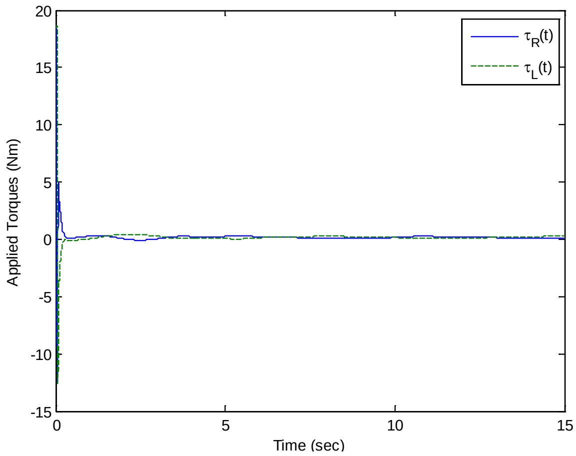

(f) $\tau_R(t)(-)$ and $\tau_L(t)(--)$.

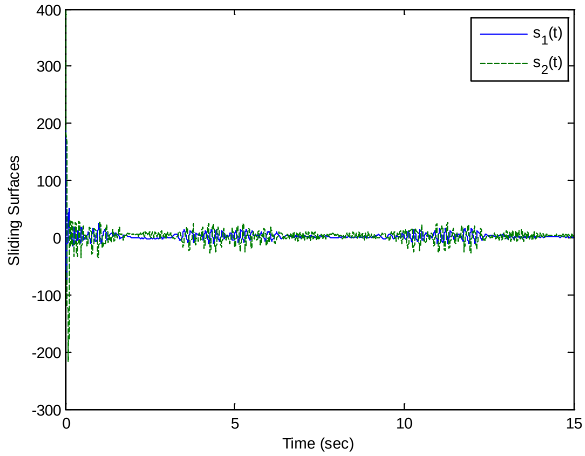

(c) $s_1(t)(-)$ and $s_2(t)(--)$.

Figure 6. Responses of the path tracking for a DDMR in the absence of uncertainties.

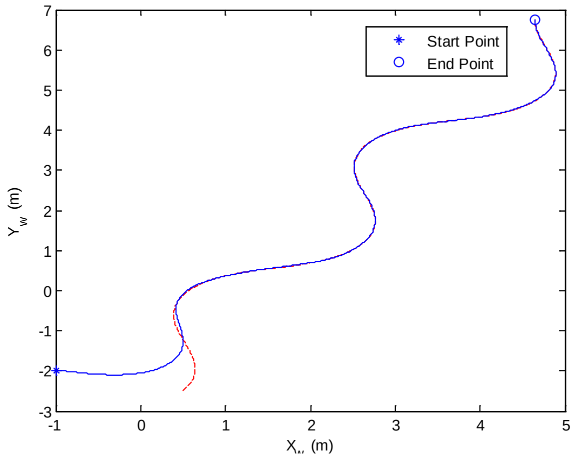

(a) $(x_w(t), y_w(t))(-)$ and $(x_r(t), y_r(t))(--)$.

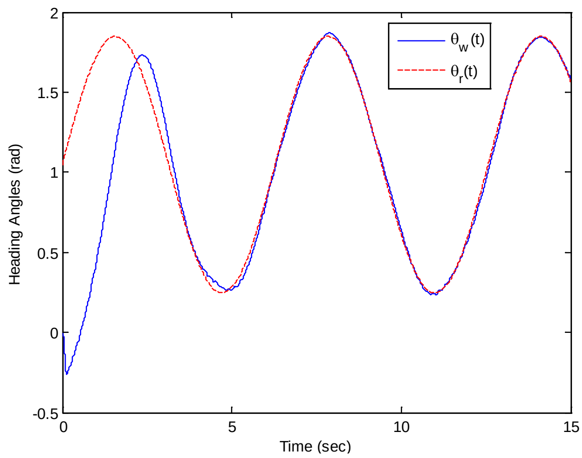

(b) $\theta_w(t)(-)$ and $\theta_r(t)(--)$.

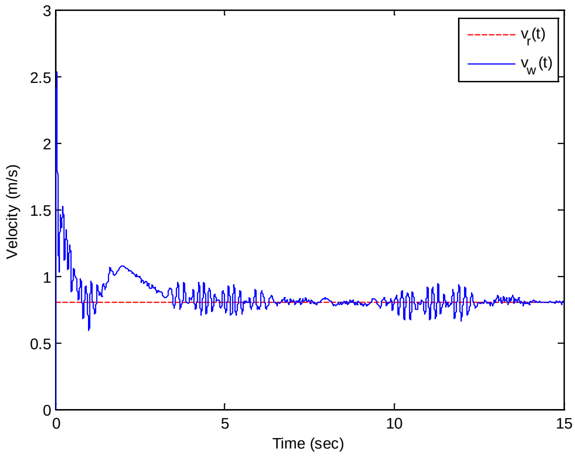

(d) $v_r(t)(--)$ and $v_w(t)(-)$.

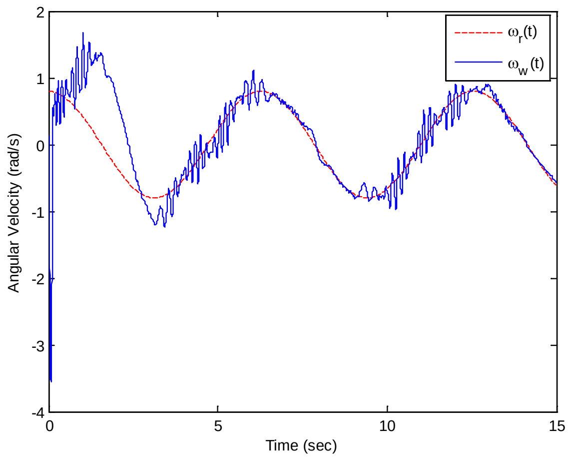

(e) $\omega_r(t)(--)$ and $\omega_w(t)(-)$.

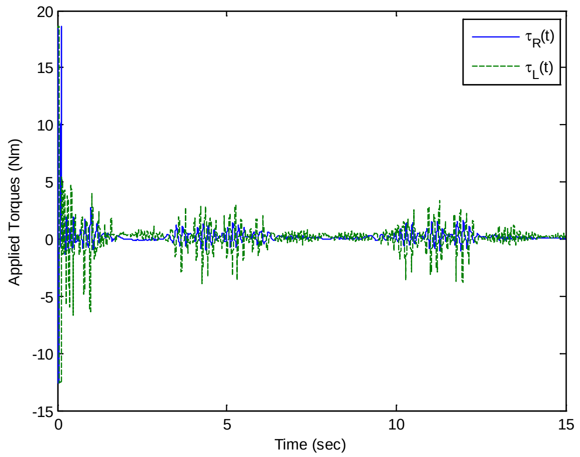

(f) $\tau_R(t)(-)$ and $\tau_L(t)(--)$.

Figure 7. Responses of the path tracking for a DDMR in the presence of uncertainties (23).

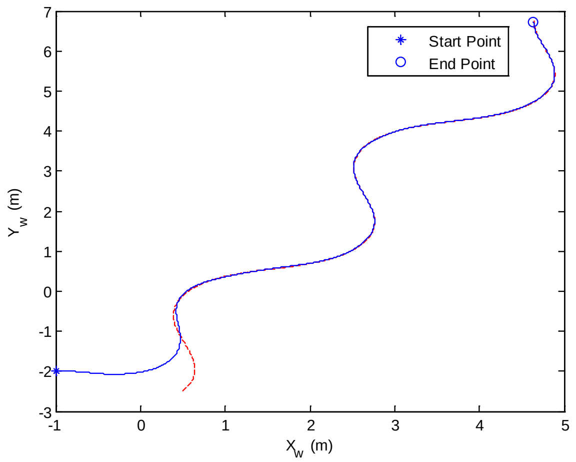

(a) $(x_w(t), y_w(t))(-)$ and $(x_r(t), y_r(t))(--)$.

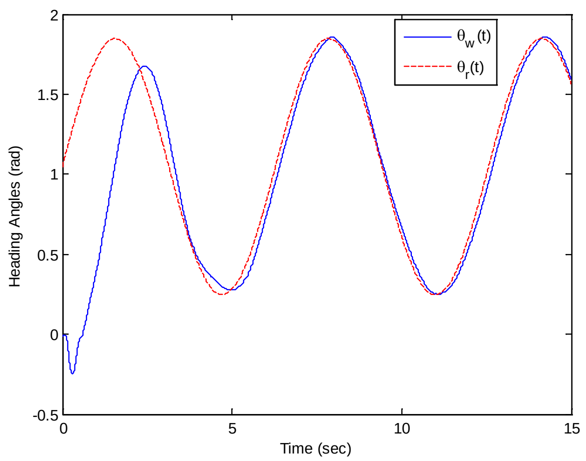

(b) $\theta_w(t)(-)$ and $\theta_r(t)(--)$.

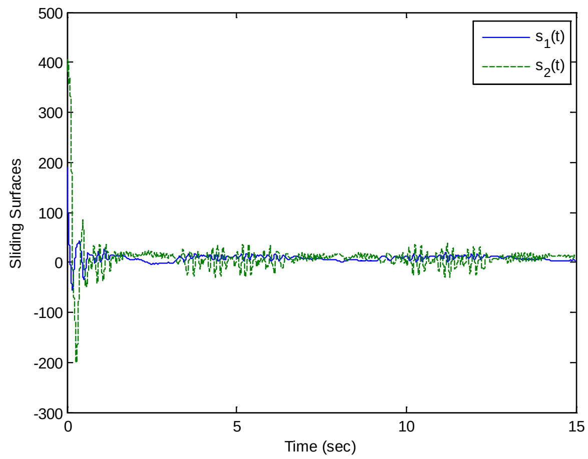

(c) $s_1(t)(-)$ and $s_2(t)(--)$.

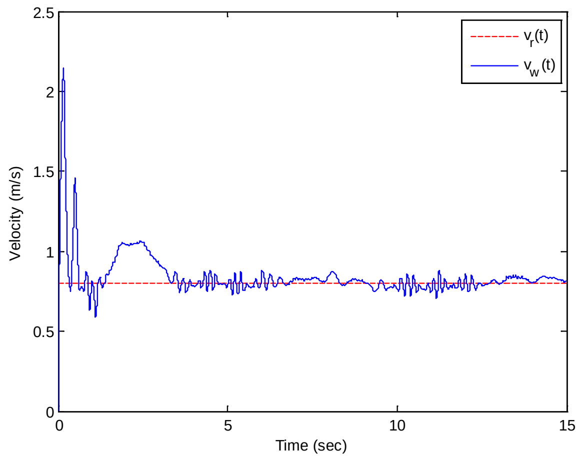

(d) $v_r(t)(--)$ and $v_w(t)(-)$.

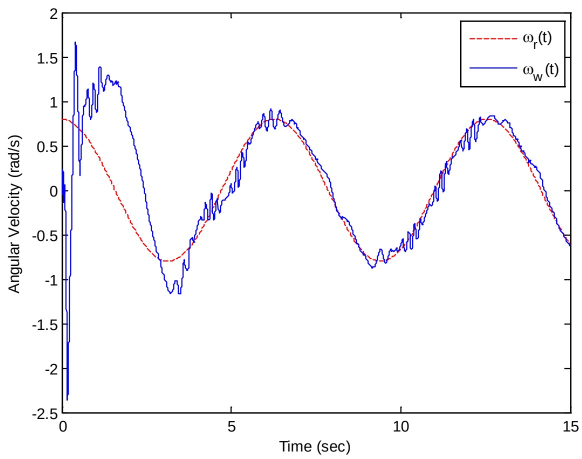

(e) $\omega_r(t)(--)$ and $\omega_w(t)(-)$.

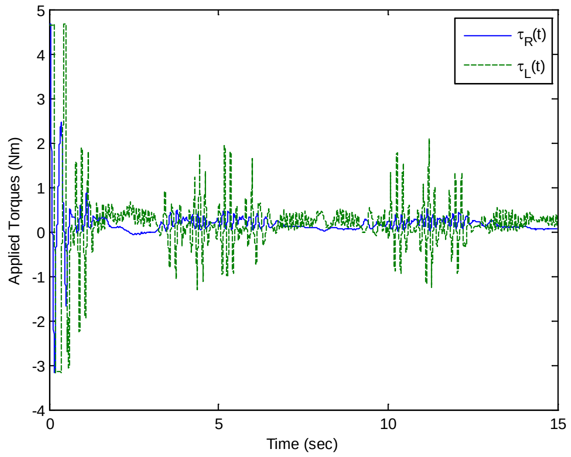

(f) $\tau_R(t)(-)$ and $\tau_L(t)(--)$.

Figure 8. Responses of the path tracking for a DDMR in the presence of uncertainties (23) and under the saturated control inputs 5*Nm*.

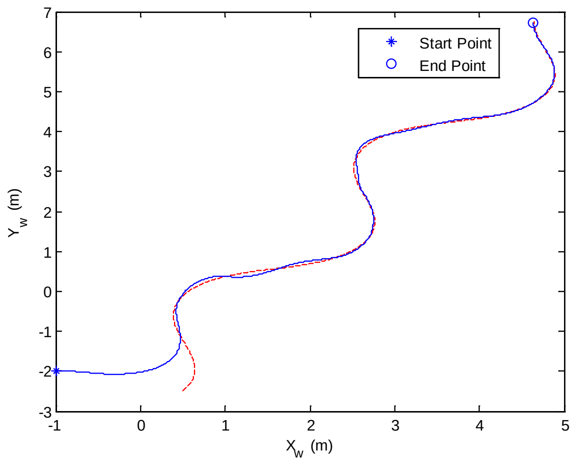

(a) $(x_w(t), y_w(t))(-)$ and $(x_r(t), y_r(t))(--)$.

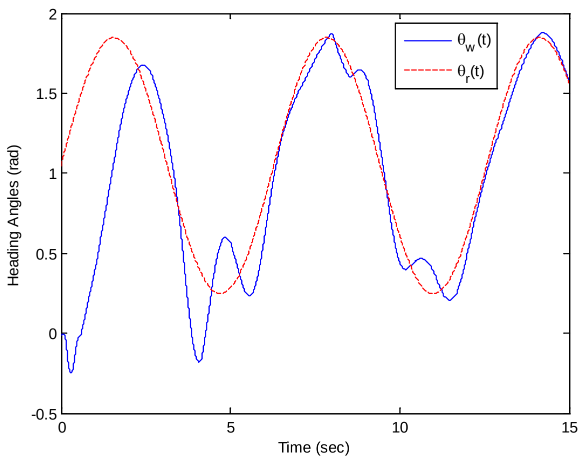

(b) $\theta_w(t)(-)$ and $\theta_r(t)(--)$.

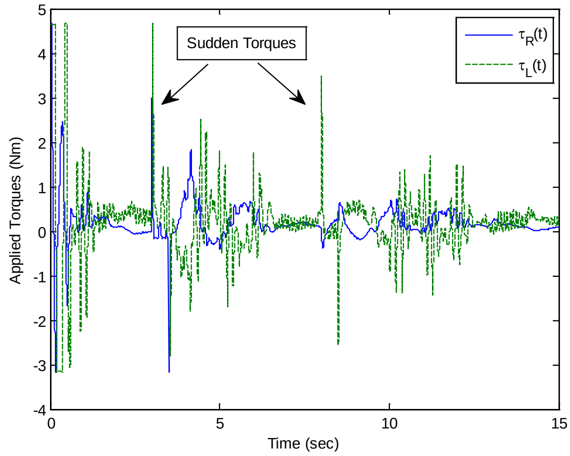

(c) $\tau_R(t)(-)$ and $\tau_L(t)(--)$.

Figure 9. Responses of the path tracking for a DDMR in the presence of uncertainties (23), saturated control inputs 5*Nm*, and the sudden torques 3 *Nm* during $t = 3 \sim 3.5$s and $t = 8 \sim 8.5$s.

From the simulation results shown in Figures 6, 7, 8 and 9, the following important observations are drawn. (i) Despite the absence (or presence) of uncertainties, saturated control input or sudden external disturbances, the proposed control technique leads to good path-tracking (cf. Figures 6(a), 7(a), 8(a) and 9(a)). (ii) The robustness of the proposed control is validated with different operating conditions (e.g., multiplicative and additive forms of uncertainties, saturated control input, and sudden external disturbances). (iii) To deal with these adverse effects, the larger output scaling factor (i.e., g_{u_1} and g_{u_2}) and the control parameters (i.e., γ_1 and γ_2) are suggested to improve the system performance. Although saturation may occur in control input, reasonable amplitudes of the saturated input still lead to satisfactory performance. (iv) Even though linear and angular velocities are not perfectly tracked when the DDMR is subjected to all kinds of uncertainties, saturated input, and external disturbances (cf. Figures 7(d), 7(e), 8(d), 8(e)), the proposed control still possesses good path tracking ability and satisfactory performance. (v)To cope with the larger uncertainties, saturated input or external disturbances, a fuzzy or neural-network model is suggested for the on-line compensation. However, this will lead to an increase in the corresponding computation load.

C ONCLUSIONS

An HDFSMC for path-tracking of a DDMR in the presence of uncertainties and friction is developed. This problem can be formulated as a virtual reference DDMR to be tracked. Based on the assigned task, direct reference input $R_1(t)$ is first planned and tracked by a NPC so that direct output of position

$Y_1(t)$ can be followed. Then the indirect reference input $R_2(t)$ is derived by Lyapunov stability theory such that the direct output of position will force the indirect output of velocity to the indirect reference input. Subsequently, the sliding surface using linear dynamics of indirect tracking errors is constructed for the design of the DFSMC. The DFSMC will make the indirect output of velocity $Y_2(t)$ track the indirect reference input $R_2(t)$. Furthermore, the stability of the closed-loop system is assured via Lyapunov stability criteria. Finally, the level of robustness and effectiveness of the proposed hierarchical control architecture (i.e., HDFSMC) is verified through computer simulations that demonstrate satisfactory performances in spite of the presence of uncertainties, saturated control inputs, and external disturbances.

REFERENCES

Yue, M., Hu, P. and Sun, W., 'Path following of a class of non-holonomic mobile with underactuated vehicle body,' *IET Control Theory and Applications*, Vol. 4, No. 10, pp. 1898–1904 (2010).

Huang, J.T., 'Adaptive tracking control of high-order nonholonomic mobile robot systems,' *IET Control Theory and Application*, Vol. 3, No. 6, pp. 681–690 (2009).

Kim, K.B. and Kim, B.K., 'Minimum-Time Trajectory for Three-Wheeled Omnidirectional Mobile Robots Following a Bounded Curvature Path With a Referenced Heading Profile,' *IEEE Transactions on Robotics*, Vol. 27, No. 4, pp. 800–808 (2011).

Rubagotti, M., Della Vedova, M.L. and Ferrara, A., 'Time-optimal sliding-mode control of a mobile robot in a dynamic environment,' *IET Control Theory and Applications*, Vol. 5, No. 16, pp. 1916–1924 (2011).

Chwa, D., 'Fuzzy Adaptive Tracking Control of Wheeled Mobile Robots With State-Dependent Kinematic and Dynamic Disturbances,' *IEEE Transactions on Fuzzy Systems*, Vol. 20, No. 3, pp. 587–593 (2012).

Chwa, D., 'Tracking Control of Differential-Drive Wheeled Mobile Robots Using a Backstepping-like Feedback Linearization,' *IEEE Transactions on System, Man and Cybernetics part A*, Vol. 40, No. 6, pp.1285–1295 (2010).

Hou, Z.G., Zou, A.M., Cheng, L. and Tan, M., 'Adaptive Control of an Electrically Driven Nonholonomic Mobile Robot via Backstepping and Fuzzy Approach,' *IEEE Transactions on Control Systems Technology*, Vol. 17, No. 4, pp. 803–815 (2009).

Fei, J.T. and Ding, H.F., 'Adaptive sliding mode control of dynamic system using RBF neural network,' *Nonlinear Dynamics*, Vol. 70, No. 2, pp. 1563–1573 (2012).

Wai, R.J. and Muthusamy, R., 'Fuzzy-Neural-Network Inherited Sliding-Mode Control for Robot Manipulator Including Actuator Dynamics,' IEEE Transactions on Neural Networks and Learning Systems, Vol. 24, No. 2, pp. 274–287 (2013).

Hwang, C.L. and Chang, L.J., 'Trajectory Tracking and Obstacle Avoidance of Car-Like Mobile Robots in an Intelligent Space Using H_2/H_∞ Decentralized Control,' *IEEE/ASME Transactions on Mechatronics*, Vol. 12, No. 3, pp. 345–352 (2007).

Kanayama, Y., Kimura, Y., Miyazaki, F. and Noguchi, T., 'A stable tracking control method for an autonomous mobile robot,' *In Proceedings of the Conference of IEEE ICRA*, Cincinnati, USA, May 13-18, pp. 384-389 (1990)

Fierro, R. and Lewis, F.L., 'Control of a Nonholonomic Mobile Robot: Backstepping Kinematics into Dynamics using Neural Networks,' *Journal of Robotic System*, Vol. 14, No. 3, pp. 149–163 (1997).

Mehrjerdi, H., Saad, M. and Ghommam, J., 'Hierarchical Fuzzy Cooperative Control and Path Following for a Team of Mobile Robots,' *IEEE/ASME Transactions on Mechatronics*, Vol. 16, No. 5, pp. 907–917 (2011).

Kwon, J.W. and Chwa, D., 'Hierarchical Formation Control Based on a Vector Field Method for Wheeled Mobile Robots,' *IEEE Transactions on Robotics*, Vol. 28, No. 6, pp. 1335–1345 (2012).

Sadati, N. and Ramezani, M.H., 'Novel interaction prediction approach to hierarchical control of large-scale systems,' *IET Control Theory and Applications*, Vol. 4, No. 2, pp. 228–243 (2010).

Goulet, J.F., De Silva, C.W., Modi, V.J. and Misra, A.K., 'Hierarchical Fuzzy Logic Control of a Manipulator With Slewing and Deployable Links,' *Journal of Vibration and Control*, Vol. 7, No. 7, pp. 1049–1086 (2001).

Qian, D., Yi, J. and Zhao, D., 'Control of a Class of Underactuated Systems with Saturation Using Hierarchical Sliding Mode,' *In Proceedings of the Conference of IEEE ICRA*, Pasadena, CA, May 19-23, pp. 2429–2434 (2008).

Drakunov, S.V. and Reyhanoglu, M., 'Hierarchical sliding mode observers for distributed parameter systems,' *Journal of Vibration and Control*, Vol. 17, No. 10, pp. 1441–1453 (2010).

Darvishzadeh, S., Rahmati, A. and Abrishamifar, A., 'Hierarchical sliding mode control of paralleling single-phase UPS inverters,' *In Proceedings of the 3rd Conference of IEEE PEDSTC*. Tehran, February pp. 15-16, 164–169 (2012).

Wang, W., Liu, X.D. and Yi, J.Q., 'Structure design of two types of sliding-mode controllers for a class of underactuated mechanical systems,' *IET*

Control Theory and Applications, Vol. 1, No. 1, pp. 163–172 (2007).
Fierro, R. and Lewis, F.L., 'Control of a nonholonomic mobile robot using neural networks,' *IEEE Transactions on Neural Networks*, Vol. 9, No. 4, pp. 389–400 (1998).
Egerstedt, M., Hu, X., and Stotsky, A., 'Control of mobile platforms using a virtual vehicle approach,' *IEEE Transactions on Automatic Control*, Vol. 46, No. 11, pp. 1777–1782 (2010).
Khalil, H.K. Nonlinear Systems, Prentice-Hall 2nd Ed. (1996)
Hwang, C.L., Chang, L.J. and Yu, Y.S., 'Network-based fuzzy decentralized sliding-mode control for car-like mobile robots,' *IEEE Transactions on Industrial Electronics*, Vol. 54, No. 1, pp. 574-585 (2007).

APPENDIXES

Appendix A (*The proof of Lemma 1*):

Without ambiguity, the arguments of variable are omitted. At beginning, the following Lyapunov function $V_1 = \left(e_1^2 + e_2^2\right)/2 + \left(1 - \cos e_3\right) \geq 0$ is defined. Taking its time derivative with the substitution of (11), (12) and (13) gives the following result:

$$\begin{aligned} \dot{V}_1 &= e_1\dot{e}_1 + e_2\dot{e}_2 + \dot{e}_3 \sin e_3 \\ &= -\gamma_1 e_1^2 - \gamma_2 e_2^2 \sin^2 e_3 \\ &\leq 0 \end{aligned} \tag{A1}$$

Consequently, it is concluded e_1, e_2 and e_3 are UUB. From (A1) and (11), it implies e_1, e_2 and $e_3 \in L_\infty \cap L_2$ (i.e., bounded and square integrable) together with $\dot{e}_1, \dot{e}_2$ and $\dot{e}_3 \in L_\infty$. Using Barbalat's lemma, it is shown e_1, e_2 and e_3 will asymptotically converge to zero as $t \to \infty$.

Q.E.D

Appendix B (*The proof of Theorem 1*):

Likewise, the Lyapunov function $V_2 = S^T S/2 = \left(s_1^2 + s_2^2\right)/2 > 0$ as $s_1 \neq 0$ or $s_2 \neq 0$, is defined. Taking its time derivative with substitution of (16), (18)-(21) yields the following result:

$$\begin{aligned} \dot{V}_2 &= s_1\dot{s}_1 + s_2\dot{s}_2 \\ &= s_1\left\{k_{p_1}\left[\dot{v}_r - \frac{r}{2}\begin{pmatrix} a_4 + a_5 + (b_{41} + b_{51})u_1 \\ +(b_{42} + b_{52})u_2 + c_4 + c_5 \end{pmatrix}\right] + k_{i_1} e_v\right\} \\ &+ s_2\left\{k_{p_2}\left[\dot{\omega}_r - \frac{r}{L}\begin{pmatrix} a_4 - a_5 + (b_{41} - b_{51})u_1 \\ +(b_{42} - b_{52})u_2 + c_4 - c_5 \end{pmatrix}\right] + k_{i_2} e_w\right\} \\ &\leq |s_1|\, h_1 - \tilde{b}_1 u_1 + |s_2|\, h_2 - \tilde{b}_2 u_2 \\ &= |s_1|\, h_1 - \left|\tilde{b}_1\right| g_{u_1} s_1^2 - |s_1|\left|\tilde{b}_1\right| g_{u_1} \Delta_1 \\ &+ |s_2|\, h_2 - \left|\tilde{b}_2\right| g_{u_2} s_2^2 - |s_2|\left|\tilde{b}_2\right| g_{u_2} \Delta_2 \\ &\leq -\left(\lambda_1 |s_1| + \lambda_2 |s_2|\right) \leq -\lambda\sqrt{s_1^2 + s_2^2} = -\lambda\sqrt{2V_2} \end{aligned} \tag{B1}$$

where $\lambda = \min\left\{\lambda_1, \lambda_2\right\}$. Then, the solution of inequality (B1) for the initial time t_0 and the initial value $S(t_0)$ is described as follows:

$$t - t_0 \leq \left\|S\left(t_0\right)\right\| / \lambda \tag{B2}$$

where t stands for the time that the operating point hits the sliding surfaces (i.e., $S(t) = 0$), and $t - t_0$ denotes the finite time to approach the sliding surface. Once the operating point reaches the stable sliding surfaces (14) and (15), the tracking error asymptotically converges to zero.

Q.E.D